

## Article

# Synthesis of Piperidine Nucleosides as Conformationally Restricted Immucillin Mimics

Maria De Fenza <sup>1</sup>, Anna Esposito <sup>1</sup>, Daniele D'Alonzo <sup>1</sup> and Annalisa Guaragna <sup>2,\*</sup>

<sup>1</sup> Department of Chemical Sciences, University of Naples Federico II, Via Cintia, 80126 Naples, Italy; maria.defenza@unina.it (M.D.F.); anna.esposito5@unina.it (A.E.); dandalonzo@unina.it (D.D.)

<sup>2</sup> Department of Chemical, Materials and Production Engineering, University of Naples Federico II, Piazzale V. Tecchio 80, 80125 Naples, Italy

\* Correspondence: annalisa.guaragna@unina.it

**Abstract:** The de novo synthesis of piperidine nucleosides from our homologating agent 5,6-dihydro-1,4-dithiin is herein reported. The structure and conformation of nucleosides were conceived to faithfully resemble the well-known nucleoside drugs Immucillins H and A in their bioactive conformation. NMR analysis of the synthesized compounds confirmed that they adopt an iminosugar conformation bearing the nucleobases and the hydroxyl groups in the appropriate orientation.

**Keywords:** immucillins; nucleoside analogues; de novo synthesis; iminosugars; biomimetics; conformationally restricted nucleosides; piperidine nucleosides; polymer-supported triphenyl phosphine



**Citation:** De Fenza, M.; Esposito, A.; D'Alonzo, D.; Guaragna, A. Synthesis of Piperidine Nucleosides as Conformationally Restricted Immucillin Mimics. *Molecules* **2021**, *26*, 1652. <https://doi.org/10.3390/molecules26061652>

Academic Editor: Pierangela Ciuffreda

Received: 25 February 2021

Accepted: 11 March 2021

Published: 16 March 2021

**Publisher's Note:** MDPI stays neutral with regard to jurisdictional claims in published maps and institutional affiliations.



**Copyright:** © 2021 by the authors. Licensee MDPI, Basel, Switzerland. This article is an open access article distributed under the terms and conditions of the Creative Commons Attribution (CC BY) license (<https://creativecommons.org/licenses/by/4.0/>).

## 1. Introduction

The modulation of the activity of carbohydrate processing enzymes represents an important therapeutic target, given the involvement of these proteins in a plethora of metabolic events causing a variety of diverse pathologies [1–3]. Over the last decades, intense efforts have been focused on the identification of inhibitors or enhancers of such enzymes [1,4–7] with promising therapeutic applications for the treatment of viral infections [8,9], cancer [10], diabetes [11], tuberculosis, lysosomal storage diseases [12], and parasitic protozoa [13]. An illustrative example in this area is represented by the class of iminosugars [4,5,7,14], glycomimetics (carbohydrate analogues) having the ring oxygen replaced by an amino group. Iminosugars are able to mimic the transition state of carbohydrate hydrolysis or transfer [15] (involving, in both cases, an upcoming glycosyl oxycarbenium cation), therefore interfering with the activity of carbohydrate-processing enzymes, such as glycosidases and glycosyltransferases [16]. Some among the most important examples of iminosugars include polyhydroxylated piperidines Miglitol, Miglustat, and Migalastat (Figure 1), which are FDA-approved drugs for the treatment of type 2 diabetes [17], Gaucher [18] and Niemann-Pick type C [19], and Fabry disease [20], respectively. Piperidine iminosugars belonging to the unnatural L-series (L-iminosugars) also exhibit pharmacological properties, such as in the case of L-DGJ [21], L-NBDNJ [22] (Figure 1), and its congeners [23,24]. Similarly, iminosugars with a pyrrolidine skeleton (in both enantiomeric series) have been found to hold excellent glycomimetic properties, as in the case of naturally occurring Radicamine A and B [25], 2,5-dideoxy-2,5-imino-D-mannitol (D-DMDP), 1,4-dideoxy-1,4-imino-D-arabinitol (D-DAB-1) (Figure 1), and their structurally related compounds [26,27]. Polyhydroxylated pyrrolidine scaffolds can also be recognized in the structure of Immucillins, which are chemically stable 9-deazapurine C-nucleoside analogues endowed with a variety of therapeutic applications, ranging from the treatment of cancer and autoimmune disorders to parasitic and viral infections [28]. Immucillin-A (1, Imm-A, also known as BCX4430 or Galidesivir, Figure 2) has demonstrated to be active in in vivo models against a variety of RNA-dependent RNA polymerases (RdRp)-based pathogens, including Ebola, Marburg, Yellow Fever, and Zika viruses [29,30].

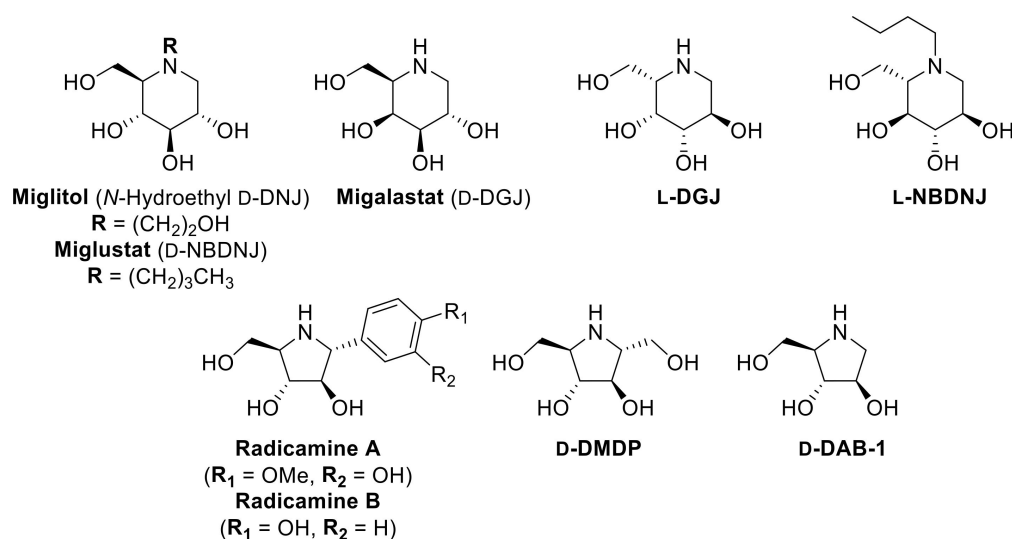


**Figure 1.** Pyrrolidine and piperidine iminosugars.

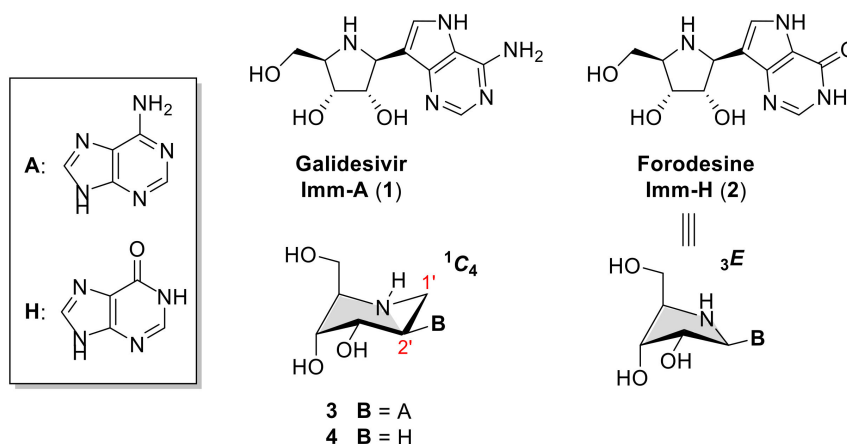


**Figure 2.** Immucillins A and H (1 and 2) and their conformationally restricted mimics 3 and 4.

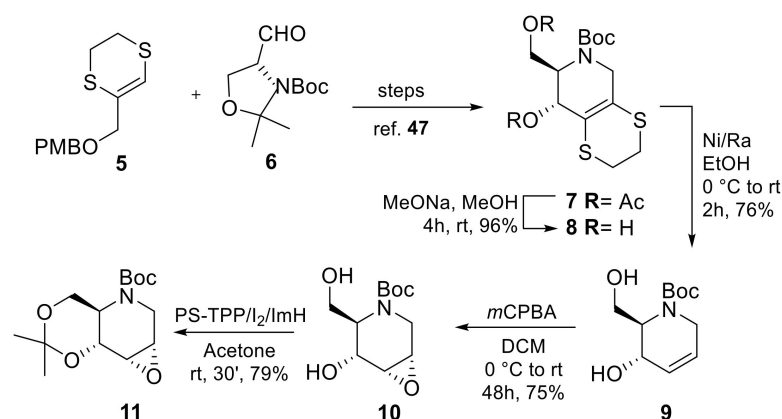
The molecule has exerted a broad-spectrum activity *in vitro* against more than 20 RNA viruses belonging to nine different families, such as flaviviruses, filoviruses and also bunyaviruses, togaviruses, paramyxoviruses, coronaviruses, and arenaviruses [31]. Lately, clinical studies have been undertaken to explore the safety and antiviral properties of Galidesivir in patients with COVID-19 [32,33]. On the other side, Immucillin H (2, Imm-H, also known as Forodesine or Mundesine, Figure 2), which is the result of a rational design process and has been at the core of intense kinetic investigations by Schramm et al., is a picomolar inhibitor of bovine and human purine nucleoside phosphorylases [34,35] (PNP, E.C. 2.4.2.1). PNP is a ubiquitous nucleoside processing enzyme essential for DNA and RNA synthesis and it is involved in the reversible phosphorolysis of purine nucleosides to the corresponding bases and (deoxy)ribose- $\alpha$ -1-phosphate. Based on the observation that PNP inhibition stops the growth of activated T-cells, Immucillin-H has been identified as a key candidate for the treatment of leukemia and autoimmune diseases [36].

Over the last decades, further design endeavours have led to the identification of a new generation of Imm-H related PNP inhibitors, endowed with an even higher potency than the parent pyrrolidine nucleoside [37]. All these inhibitors shared an increase of conformational freedom degrees compared with Imm-H [37]. With the aim to provide an alternative strategy to PNP inhibitors, we conceived to replace the pyrrolidine scaffold with a conformationally more restricted biomimetic system. Our approach exploits the well-known finding that the quality of host-guest interactions benefits from the increase

in the preorganization of the guest, since no entropy penalty is involved in the binding process. As demonstrative examples, conformationally restricted nucleosides bearing a six-membered sugar unit have already been found to hold an excellent biomimetic potential in various therapeutic contexts [38,39], as a result of the resemblance of natural ribofuranosyl nucleosides in their bioactive conformations [40]. Accordingly, following our longstanding interest in the identification of conformationally restricted molecules with biomimetic properties [39,41–46], we undertook the synthesis of novel Immucillin-A and Immucillin-H analogues, i.e., polyhydroxylated piperidine nucleosides **3** and **4** (Figure 2). Our goal was to replace the five membered pyrrolidine scaffold of the drug candidates with a biomimetic six-membered unit. Indeed, among the two chair conformations that **3** and **4** are expected to be able to adopt, the  ${}^1C_4$  form mimics the bioactive  ${}^3E$  conformation of Immucillins when bound to the PNP active site [37]. On this basis, this preliminary study is first aimed to tune up the synthetic path using natural nucleobases as model aglycones, in view of the synthesis of the congeners equipped with the more complex 9-deazapurine nucleobases. Indeed, differently from pyrrolidine nucleosides, move of the nucleobase from C1' to C2' in piperidine nucleosides, required for Immucillin biomimicry, allows to install natural nucleobases without affecting the structural integrity of the molecule. In addition, the analysis of the conformational preferences of **3** and **4** is herein performed to ascertain the biomimetic properties of this novel class of nucleoside analogues.

## 2. Results and Discussion

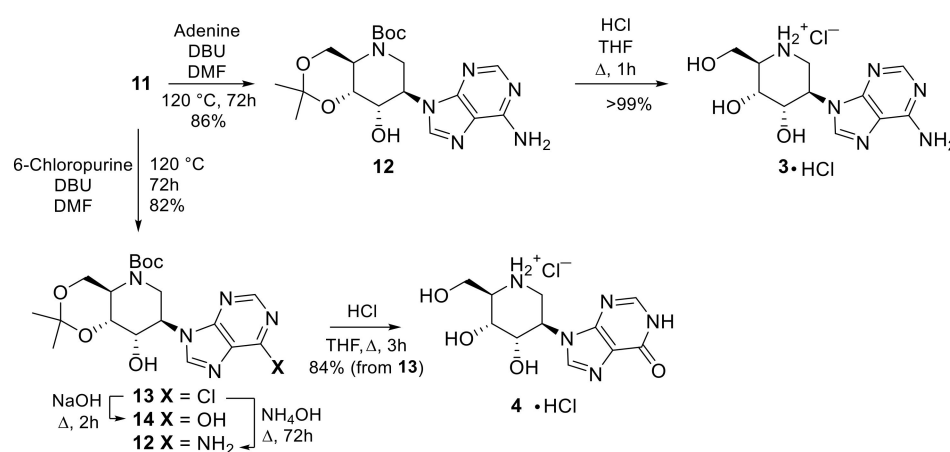
The synthesis of nucleosides **3** and **4** was achieved from heterocyclic system **7**, in turn obtained in a few steps by dithiin **5** and (*R*)-Garner aldehyde (**6**) (Scheme 1), using a similar synthetic sequence previously enabling the synthesis of unnatural L-iminosugars [22,23,47]. Deacetylation of **7** under Zemplén conditions (NaOMe, MeOH) quantitatively afforded **8** (96%), which was then treated with Raney<sup>®</sup>-Ni in EtOH to cleave the dithioethylene bridge, yielding olefin **9** (76% yield). Stereoselective 4-OH-directed epoxidation of **9**, using *m*CPBA in CH<sub>2</sub>Cl<sub>2</sub> led, as expected, exclusively to *cis* oxirane **10** (75% yield). In the subsequent ketalization step of OH groups in **10**, we used an alternative procedure to the standard protocol (PTSA, 2,2-dimethoxypropane, 2-methoxypropene) [48], in order to avoid strictly anhydrous conditions, which are typically required to limit by-product formation derived from acid-catalysed oxirane ring opening. Exploiting our longstanding expertise in the field [23,49–53], we chose the procedure involving the use of polymer-supported triphenyl phosphine (PS-TPP)/I<sub>2</sub>/imidazole (ImH) system as the activating agent for the protection reaction, using acetone as the acetonide source. In this case, the reaction involves the activation of acetone by the triphenylphosphonium iodide and the subsequent double attack by the diol to the activated ketone. Challenging for our synthetic target, PS-TPP/I<sub>2</sub>/ImH is also reported to enable epoxide ring opening, to provide the corresponding iodohydrins [54].



**Scheme 1.** *De novo* approach to *cis* epoxide **11**.

However, in our hands, the addition of **10** to a suspension of the premixed activating agent in the anhydrous acetone provided, already after 1 h at room temperature, the corresponding 4',6'-*O*-isopropylidene derivative **11** with no traces of other byproducts. The pure ketal **11** could be isolated after a simple filtration of the reaction mixture, increasing the synthetic benefits of the procedure.

With the fully protected epoxide **11** in hand, piperidine nucleosides were eventually obtained, as already reported for similar substrates [42]. By virtue of the locked conformation of compound **11**, the treatment of the latter with DBU and adenine in anhydrous DMF at 120 °C (Scheme 2) only led to the epoxide ring opening by the nucleobase at the desired C2 axial position, affording regioselectively the corresponding protected alditol-like nucleoside **12**, additionally in a very good yield (86%). Under the same coupling conditions, the treatment of **11** with 6-chloropurine provided a mixture of chloropurine and hypoxanthine-containing nucleosides **13** (82%) and **14** (18%), respectively. Alternatively, the same reaction carried out replacing DBU with NaH in DMF at room temperature yielded 6-chloropurine nucleoside as the only observed product. The quantitative conversion of **13** into **14** could be then obtained by the treatment with a refluxing 0.5 M NaOH solution, while the corresponding adenosine derivative **12** could be obtained by the treatment of **13** with conc. NH<sub>4</sub>OH at reflux temperature. Eventually, the subsequent addition of 2 M HCl to crude nucleosides **12** and **14** allowed both isopropylidene and Boc groups removal, providing the corresponding nucleosides **3** and **4** as HCl salts (**3**: > 99% from **12**; **4**: 84% from **13**).



**Scheme 2.** Synthesis of Immucillin H and A analogues **3** and **4**.

The NMR analysis of nucleosides **3** and **4** confirmed the formation of N9-C2' bonds, as revealed by HMBC correlations between H-2' of the piperidine and the C-4 of purines. Furthermore, 1D and 2D spectra strongly suggested that the desired conformations with equatorially oriented nucleobases were adopted by both nucleosides (Figure 3). Indeed, <sup>1</sup>H NMR analysis provided large coupling constants between H-1'/H-2' (10.8 Hz in both cases) and H-2'/H-3' (**3**: 10.2 Hz; **4**: 10.0 Hz), as well as relatively small coupling constants between H-4'/H-5' (**3**: 3.1 Hz; **4**: 3.4 Hz), which are responsible for the *trans* diequatorial interaction between the two protons. On the other hand, the NOESY analysis revealed dipolar interactions between the axially oriented H-1' and H-6'a (Figure 3).

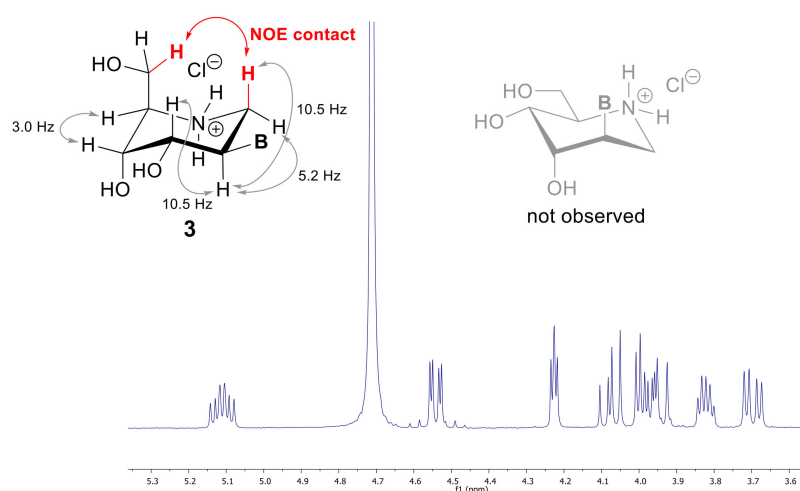


**Figure 3.**  $^1\text{H}$  NMR analysis of **3** HCl.

The observed piperidine conformation is opposite to the  $^4\text{C}_1$  form (axially oriented nucleobase) adopted by *altro*-configured nucleosides having a ring oxygen and more generally by the majority of biomimetic hexitol nucleosides [40,55]. Conversely, the conformation of **3** and **4** is in line with those adopted by cyclohexanyl nucleosides, having a methylene group in place of ring heteroatom [42,56]. In agreement with previous studies on both hexitol and cyclohexanyl nucleosides [56], it is conceivable to hypothesize that the conformation of piperidine nucleosides is adopted to relieve the 1,3-diaxial strains involving the nucleobase and hydrogen atoms from C4 and the protonated amino group in the  $^4\text{C}_1$  conformer (Figure 3).

Having equatorially oriented nucleobases, nucleosides **3** and **4** hold the conformational requirements to mimic the  $^3E$  pyrrolidine ring puckering of Immucillins H and A. Based on these data, the piperidine core can be therefore considered as an appropriate scaffold for the construction of preorganized Immucillin analogues.

### 3. Materials and Methods

#### 3.1. Chemistry

All chemicals and solvents were purchased with the highest degree of purity (Sigma-Aldrich, Darmstadt, Germany; Alfa Aesar, Karlsruhe, Germany; VWR, Milan, Italy) and used without further purification. The reactions were monitored by TLC (precoated silica gel plate F254, Merck, Darmstadt, Germany) and the products were detected by exposure to ultraviolet radiation, iodine vapor, and chromic mixture. Column chromatography: Merck Kieselgel 60 (70–230 mesh). The purity of compounds was determined by CHNS analysis and was  $\geq 95\%$  in all cases. NMR spectra were acquired on NMR spectrometers operating at 200 MHz (Varian, Palo Alto, California), 400 MHz (Bruker AVANCE, Billerica, Massachusetts, US) or 500 MHz (Varian Inova, Palo Alto, California, US), using  $\text{CDCl}_3$  solutions unless otherwise specified. Coupling constant values ( $J$ ) were reported in Hz, details in Supplementary Materials.

#### 3.2. Procedures for the Synthesis of **3**–**13**

**Bicyclic Compound 8.** MeONa (16 mg, 0.30 mmol) was added to a stirring solution of **7** [47] (0.12 g, 0.30 mmol) in MeOH (2.0 mL). The mixture was stirred for 4 h at room temperature and then neutralized with a few drops of acetic acid. Then, solvent removal under reduced pressure and chromatography of the crude residue over silica gel (hexane/EtOAc = 6/4) provided pure **2** (92 mg, 96% yield) as a colorless oil.  $[\alpha]_D^{25} + 47.2$  ( $c$  0.22, MeOH).  $^1\text{H}$  NMR (200 MHz): 1.48 (s, 9H), 1.68 (bs 2H), 3.19–3.26 (m, 4H), 3.56–3.68 (m, 3H), 3.90 (bs, 1H), 4.19–4.32 (m, 1H), 4.48–4.56 (m, 1H).  $^{13}\text{C}$  NMR (50 MHz): 27.8, 28.2,

44.8, 58.3, 60.6, 68.0, 81.0, 119.9, 121.5, 145.9, 155.7 ppm. Anal. calcd for C<sub>13</sub>H<sub>21</sub>NS<sub>2</sub>O<sub>4</sub>: C 48.88, H 6.63, N 4.38, S 20.07. Found: C 48.98, H 6.61, N 4.39, S 20.02.

**Diol 9.** To a suspension of Raney-Ni (W2) (0.90 g, wet) in EtOH (1 mL) a solution of bicycle piperidine **8** (90 mg, 0.28 mmol) in the same solvent (3 mL) at 0 °C was added. The suspension was stirred for 2 h at room temperature, then the solid was filtered off and washed with EtOH. The filtrate was concentrated under reduced pressure providing the crude residue whose chromatography over silica gel (hexane/acetone = 6/4) gave pure **9** (49 mg, 76% yield) as a colorless oil.  $[\alpha]_D^{25} + 87.8$  (c 0.85, CHCl<sub>3</sub>). NMR data for **9** were consistent with those reported elsewhere [57]. Anal. calcd for C<sub>11</sub>H<sub>19</sub>NO<sub>4</sub>: C 57.63, H 8.35, N 6.11. Found: C 57.73, H 8.83, N 6.10.

**Epoxide 10.** To a stirred solution of diol **9** (49 mg, 0.21 mmol) in anhydrous CH<sub>2</sub>Cl<sub>2</sub> (2 mL), *m*-CPBA (43 mg, 0.25 mmol) was added at 0 °C. The mixture was stirred for 48 h at room temperature and then aq. NaHCO<sub>3</sub> was added and the mixture was extracted with CH<sub>2</sub>Cl<sub>2</sub>. The organic layer was dried (Na<sub>2</sub>SO<sub>4</sub>) and the solvent evaporated under reduced pressure. Chromatography of the crude residue over silica gel (hexane/EtOAc = 1:9) afforded pure **10** (40 mg, 75% yield): oily,  $[\alpha]_D^{25} + 14.3$  (c 1.0, CHCl<sub>3</sub>). <sup>1</sup>H NMR (400 MHz): δ 1.46 (s, 9H), 2.20 (bs, D<sub>2</sub>O exchange, 2H), 3.31 (bs, 1H), 3.39 (bd, *J* = 3.8, 1H), 3.46 (t, *J* = 4.5, 1H), 3.59 (d, *J* = 8.0, 11.3, 1H), 3.68 (dd, *J* = 6.0, 11.3, 1H), 3.94 (dd, *J* = 1.4, 4.5, 1H), 4.18 (bt, *J* = 6.0, 1H), 4.28 (bs, 1H). <sup>13</sup>C NMR (100 MHz): 24.3, 47.5, 48.3, 52.9, 56.4, 58.5, 7.2, 76.9, 152.4 ppm. Anal. calcd for C<sub>11</sub>H<sub>19</sub>NO<sub>5</sub>: C 53.87, H 7.81, N 5.71. Found: C 53.96, H 7.79, N 5.72.

**Protected Epoxide 11.** To a magnetically stirred solution of polymer supported triphenylphosphine (PS-TPP; 100–200 mesh, extent of labeling: ~3 mmol/g triphenylphosphine loading) (80 mg, ~0.24 mmol) in anhydrous acetone (0.5 mL) at room temperature, a solution of I<sub>2</sub> (60 mg, 0.24 mmol) in the same solvent (0.7 mL) was added dropwise in the dark and under dry N<sub>2</sub> atmosphere. Subsequently imidazole (32 mg, 0.48 mmol) was added and after 15 min **10** (40 mg, 0.16 mmol) was added in one portion to the suspension. TLC monitoring showed the complete consumption of starting sugar within 10 min. The resulting mixture was filtered and the solvent removed at room temperature under reduced pressure, affording **11** (36 mg, 79% yield) as a colorless oil.  $[\alpha]_D^{25} + 1.2$  (c 2.0, CHCl<sub>3</sub>). <sup>1</sup>H NMR (500 MHz, acetone-*d*<sub>6</sub>): δ 1.35 (s, 3H), 1.46 (s, 9H), 1.52 (s, 3H), 3.26 (d, *J* = 4.8, 1H), 3.31 (td, *J* = 4.8, 10.7 1H), 3.41–3.44 (m, 1H), 3.76 (d, *J* = 15.3, 1H), 3.83 (dd, *J* = 2.0, 15.3, 1H), 4.15 (t, *J* = 10.7, 1H), 4.23 (dd, *J* = 4.8, 10.7, 1H), 4.37 (d, *J* = 10.7, 1H). <sup>13</sup>C NMR (125 MHz, acetone-*d*<sub>6</sub>): 18.6, 27.5, 29.7, 42.6, 51.0, 51.8, 62.4, 69.5, 79.8, 98.9, 154.4 ppm. Anal. calcd for C<sub>14</sub>H<sub>23</sub>NO<sub>5</sub>: C 58.93, H 8.13, N 4.91. Found: C 59.06, H 8.1, N 4.92.

**Nucleoside 12.** Adenine (36 mg, 0.26 mmol) and epoxide **11** (35 mg, 0.12 mmol) were suspended in anhydrous DMF (0.9 mL) for 15 min, at room temperature under Ar atmosphere. Then, 1,8-diazabicyclo[5.4.0]undec-7-ene (DBU, 0.26 mmol, 39 μL) was added and the resulting mixture was heated at 90 °C and stirred for 72 h. The reaction mixture was cooled to room temperature, quenched with sat.aq. NH<sub>4</sub>Cl, and concentrated under reduced pressure. The crude residue was extracted with EtOAc and washed with brine. The organic layers were dried (Na<sub>2</sub>SO<sub>4</sub>) and the solvent evaporated under reduced pressure. Chromatography of the crude residue over silica gel (EtOAc:MeOH = 9:1) gave pure **12** (43 mg, 86% yield): oily,  $[\alpha]_D^{25} - 21.2$  (c 1.0, MeOH). <sup>1</sup>H NMR (400 MHz, CD<sub>3</sub>OD): δ 1.44 (s, 3H), 1.47 (s, 9H), 1.60 (s, 3H), 3.78 (td, *J* = 4.7, 10.5, 1H), 3.98 (dd, *J* = 5.2, 13.9, 1H), 4.03–4.12 (m, 2H), 4.34 (bt, *J* = 2.7, 1H), 4.38 (dd, *J* = 4.7, 10.5 Hz, 1H), 4.60–4.65 (m, 2H), 8.21 (s, 1H), 8.22 (s, 1H). <sup>13</sup>C NMR (100 MHz, CD<sub>3</sub>OD): 19.6, 28.5, 29.4, 42.9, 59.8, 63.9, 70.2, 70.9, 82.4, 100.7, 120.2, 141.5, 150.8, 153.8, 156.6, 157.5 ppm. Anal. calcd for C<sub>19</sub>H<sub>28</sub>N<sub>6</sub>O<sub>5</sub>: C 54.27, H 6.71, N 19.99. Found: C 54.27, H 6.73, N 20.05.

**Nucleoside 13.** 6-Chloropurine (31 mg, 0.20 mmol) and epoxide **11** (25 mg, 0.09 mmol) were suspended in anhydrous DMF (0.5 mL) at room temperature under Ar atmosphere. After 15 min, 1,8-diazobicyclo[5.4.0]undec-7-ene (DBU, 30 μL, 0.20 mmol) was added and the reaction mixture was heated at 120 °C and stirred for 72 h. Then, the reaction mixture was cooled to room temperature, quenched with NH<sub>4</sub>Cl, and concentrated under reduced

pressure. The crude residue was extracted with DCM and washed with brine. The organic layers were dried ( $\text{Na}_2\text{SO}_4$ ) and the solvent evaporated under reduced pressure. Flash chromatography of the crude residue over silica gel (AcOEt) gave pure **13** (32 mg, 82% yield): oily,  $[\alpha]_{\text{D}}^{25} + 3.3$  ( $c$  0.33, acetone).  $^1\text{H}$  NMR ( $\text{CDCl}_3$ , 500 MHz):  $\delta$  1.42 (s, 3H), 1.45 (s, 9H), 1.50 (s, 3H), 3.54 (bs, 1H), 3.67 (td,  $J = 10.5, 4.9$  Hz, 1H), 3.89 (dd,  $J = 14.3, 4.4$  Hz, 1H), 4.12 (t,  $J = 11.0$  Hz, 1H), 4.17 (dd,  $J = 3.0, 10.5$  Hz, 1H), 4.27 (dd,  $J = 14.3, 6.0$  Hz, 1H), 4.36 (t,  $J = 2.9$  Hz, 1H), 4.51 (dd,  $J = 11.5, 4.9$  Hz, 1H), 4.62–4.64 (m, 1H), 7.87 (s, 1H), 8.32 (s, 1H).  $^{13}\text{C}$  NMR (100 MHz): 19.6, 28.5, 29.3, 42.8, 49.6, 55.9, 63.0, 68.6, 69.7, 81.7, 99.4, 120.3, 137.0, 150.6, 152.6, 154.7 ppm. Anal. calcd for  $\text{C}_{19}\text{H}_{26}\text{ClN}_5\text{O}_5$ : C 51.88, H 5.96, Cl 8.06, N 15.92. Found: C 51.77, H 5.94, Cl 8.09, N 15.97.

Adenosine analogue **3**. Procedure A (from **12**). 2 M HCl (11.6 mL) was added to a solution of **12** (40 mg, 0.09 mmol) in THF (0.6 mL) and the reaction mixture was heated to reflux temperature for 1 h. Removal of the volatiles under reduced pressure and subsequent trituration with  $\text{Et}_2\text{O}$  afforded **3** as hydrochloride salt (30 mg, quant.). Procedure B (from **13**). Compound **13** (15 mg, 0.03 mmol) was treated with 13 M  $\text{NH}_4\text{OH}$  (4.5 mL). The mixture was added to a steel bomb reactor heated to reflux temperature for 72 h. The reaction was quenched by the addition of a few drops of HCl (1N) and concentrated under reduced pressure. The crude residue was then diluted with  $\text{CHCl}_3$  : MeOH = 8:2 and filtered under a silica pad. Volatiles were removed under reduced pressure to obtain **12** a white solid. As described in procedure A, THF (2 mL) and HCl 2 M (0.6 mL) were then added and the solution was heated to reflux temperature for 1 h. Removal of the solvents under reduced pressure and the subsequent trituration of the solid with  $\text{Et}_2\text{O}$  gave pure **3** as hydrochloride salt (7.0 mg, 65% yield over two steps). Data for **3**: white solid,  $[\alpha]_{\text{D}}^{25} - 8.25$  ( $c$  0.14,  $\text{H}_2\text{O}$ ).  $^1\text{H}$  NMR (400 MHz,  $\text{D}_2\text{O}$ ):  $\delta$  3.76 (dd,  $J = 5.2, 13.4$ , 1H), 3.90 (dt,  $J = 3.5, 8.8$ , 1H), 4.03 (dd,  $J = 10.5, 13.4$ , 1H), 4.07 (dd,  $J = 3.5, 12.8$ , 1H), 4.16 (dd,  $J = 8.8, 12.8$ , 1H), 4.31 (t,  $J = 3.5$  Hz, 1H), 4.62 (dd,  $J = 3.5, 10.5$ , 1H), 5.19 (td,  $J = 5.2, 10.5$ , 1H), 8.38 (s, 1H), 8.39 (s, 1H).  $^{13}\text{C}$  NMR (100 MHz,  $\text{D}_2\text{O}$ ): 39.7, 53.3, 55.8, 59.9, 65.9, 66.9, 118.9, 144.2, 144.4, 148.6, 149.9 ppm. Anal. calcd for  $\text{C}_{11}\text{H}_{17}\text{ClN}_6\text{O}_3$ : C 41.71, H 5.41, Cl 11.19, N 26.53. Found: C 41.56, H 5.39, Cl 11.24, N 26.63.

Hypoxanthine analogue **4**. Nucleoside **13** (15 mg, 0.03 mmol) was refluxed for 2 h in a 0.5 N aq NaOH (0.5 mL). Then, the reaction mixture was cooled to 0 °C and 0.5 N HCl was carefully added (0.8 mL). The solution was evaporated under reduced pressure. The crude was then dissolved in THF (0.2 mL) and then 2 M HCl (0.5 mL) was added. The reaction mixture was heated to reflux temperature for 3 h. Then, the solvent was evaporated under reduced pressure and the subsequent trituration of the solid with  $\text{Et}_2\text{O}$  gave pure **4** as hydrochloride salt (8.0 mg, 84%).  $[\alpha]_{\text{D}}^{25} + 2.8$  ( $c$  0.14,  $\text{H}_2\text{O}$ ).  $^1\text{H}$  NMR (400 MHz,  $\text{D}_2\text{O}$ ):  $\delta$  3.74 (dd,  $J = 5.1, 13.3$ , 1H), 3.89 (m, 1H), 4.02 (dd,  $J = 10.8, 13.3$ , 1H), 4.05 (dd,  $J = 3.4, 12.8$ , 1H), 4.15 (dd,  $J = 8.9, 12.8$ , 1H), 4.30 (t,  $J = 3.4$  Hz, 1H), 4.61 (dd,  $J = 3.3, 10.0$ , 1H), 5.18 (td,  $J = 5.1, 10.0$ , 1H), 8.40 (s, 1H), 8.42 (s, 1H).  $^{13}\text{C}$  NMR (100 MHz,  $\text{D}_2\text{O}$ ): 35.8, 49.1, 51.8, 55.9, 62.0, 62.8, 115.6, 123.4, 138.6, 140.5, 144.3 ppm. Anal. calcd for  $\text{C}_{11}\text{H}_{16}\text{ClN}_5\text{O}_4$ : C 41.58, H 5.08, Cl 11.16, N 22.04. Found: C 41.49, H 5.10, Cl 11.18, N 22.04.

#### 4. Conclusions

The synthesis of piperidine nucleosides **3** and **4**, acting as conformationally restricted analogues of Immucillins H and A, has been herein reported. Our approach exploits our consolidated strategy, involving the synthetic manipulation of coupling product **7** starting from our three-carbon homologating agent **5**. The stereoselective preparation of *cis* epoxide **11** and the subsequent coupling reaction in two alternative approaches with model nucleobases have enabled access to piperidine nucleosides **3** and **4** with the desired *D-altro* configuration. NMR analysis demonstrated that both compounds resemble the bioactive conformation of Immucillins H and A, as they adopt iminosugar conformations with equatorially oriented nucleobases. Further studies will be devoted to explore the suitability of our approach to introduce a variety of other heterocyclic bases for SAR analysis. Particularly, synthetic studies aimed to incorporate Immucillin-mimicking 9-deazapurine

nucleobases and in vitro assays, aimed to ascertain the pharmacological potential of all the synthesised nucleosides, are currently ongoing and will be published elsewhere.

**Supplementary Materials:** Figure S1: <sup>1</sup>H and <sup>13</sup>C NMR spectra of compound 8; Figure S2: <sup>1</sup>H and <sup>13</sup>C NMR spectra of compound 10; Figure S3: <sup>1</sup>H and <sup>13</sup>C spectra of compound 11; Figure S4: <sup>1</sup>H and <sup>13</sup>C NMR spectra of compound 12; Figure S5: <sup>1</sup>H and <sup>13</sup>C NMR spectra of compound 13; Figure S6: <sup>1</sup>H and <sup>13</sup>C NMR spectra of compound 3; Figure S7: <sup>1</sup>H and <sup>13</sup>C NMR spectra of compound 4.

**Author Contributions:** Conceptualization, A.G. and D.D.; methodology, A.E.; software, A.E.; validation, M.D.F. and D.D.; formal analysis, M.D.F.; investigation, M.D.F.; data curation, A.E.; writing—original draft preparation, A.G.; writing—review and editing, D.D., M.D.F. and A.E.; supervision, D.D.; project administration, A.G.; funding acquisition, A.G. All authors have read and agreed to the published version of the manuscript.

**Funding:** This research received no external funding.

**Institutional Review Board Statement:** Not applicable.

**Informed Consent Statement:** Not applicable.

**Data Availability Statement:** The data presented in this study are available within the article and in the Supplementary Materials section.

**Conflicts of Interest:** The authors declare no conflict of interest.

## References

1. Varki, A.; Cummings, R.D.; Esko, J.D.; Stanley, P.; Hart, G.W.; Aebi, M.; Darvill, A.G.; Kinoshita, T.; Packer, N.H.; Prestegard, J.H.; et al. *Essentials of Glycobiology*, 3rd ed.; Cold Spring Harbor Laboratory Press: Cold Spring Harbor, NY, USA, 2009.
2. Gloster, T.M.; Vocadlo, D.J. Developing inhibitors of glycan processing enzymes as tools for enabling glycobiology. *Nat. Chem. Biol.* **2012**, *8*, 683–694. [[CrossRef](#)] [[PubMed](#)]
3. Stütz, A.E.; Wrodnigg, T.M. Carbohydrate-processing enzymes of the lysosome: Diseases caused by misfolded mutants and sugar mimetics as correcting pharmacological chaperones. *Adv. Carbohydr. Chem. Biochem.* **2016**, *73*, 225–302. [[PubMed](#)]
4. Compain, P.; Martin, O.R. *Iminosugars: From Synthesis to Therapeutic Applications*, 1st ed.; John Wiley & Sons, Ltd: Chichester, UK, 2007.
5. Horne, G.; Wilson, F.X.; Tinsley, J.; Williams, D.H.; Storer, R. Iminosugars past, present and future: Medicines for tomorrow. *Drug Discov. Today* **2011**, *16*, 107–118. [[CrossRef](#)]
6. Chao, L.; Jongkees, S. High-Throughput approaches in carbohydrate-active enzymology: Glycosidase and glycosyl transferase inhibitors, evolution, and discovery. *Angew. Chem. Int. Ed.* **2019**, *58*, 12750–12760. [[CrossRef](#)] [[PubMed](#)]
7. Nash, R.J.; Kato, A.; Yu, C.-Y.; Fleet, G.W. Iminosugars as therapeutic agents: Recent advances and promising trends. *Future Med. Chem.* **2011**, *3*, 1513–1521. [[CrossRef](#)]
8. Alonzi, D.S.; Scott, K.A.; Dwek, R.A.; Zitzmann, N. Iminosugar antivirals: The therapeutic sweet spot. *Biochem. Soc. Trans.* **2017**, *45*, 571–582. [[CrossRef](#)]
9. Evans DeWald, L.; Starr, C.; Butters, T.; Treston, A.; Warfield, K.L. Iminosugars: A host-targeted approach to combat Flaviviridae infections. *Antiviral Res.* **2020**, *184*, 104881. [[CrossRef](#)] [[PubMed](#)]
10. Wrodnigg, T.; Steiner, A.; Ueberbacher, B. Natural and synthetic iminosugars as carbohydrate processing enzyme inhibitors for cancer therapy. *Anticancer. Agents Med. Chem.* **2008**, *8*, 77–85. [[CrossRef](#)] [[PubMed](#)]
11. Derosa, G.; Maffioli, P. Mini-special issue paper management of diabetic patients with hypoglycemic agents  $\alpha$ -glucosidase inhibitors and their use in clinical practice. *Arch. Med. Sci.* **2012**, *5*, 899–906. [[CrossRef](#)]
12. Platt, F.M.; D’Azzo, A.; Davidson, B.L.; Neufeld, E.F.; Tiffit, C.J. Lysosomal storage diseases. *Nat. Rev. Dis. Prim.* **2018**, *4*, 27. [[CrossRef](#)]
13. Cheviet, T.; Lefebvre-Tournier, I.; Wein, S.; Peyrottes, S. Plasmodium purine metabolism and its inhibition by nucleoside and nucleotide analogues. *J. Med. Chem.* **2019**, *62*, 8365–8391. [[CrossRef](#)]
14. D’Alonzo, D.; Guaragna, A.; Palumbo, G. Glycomimetics at the mirror: Medicinal chemistry of L-iminosugars. *Curr. Med. Chem.* **2009**, *16*, 473–505. [[CrossRef](#)]
15. Gloster, T.M.; Davies, G.J. Glycosidase inhibition: Assessing mimicry of the transition state. *Org. Biomol. Chem.* **2010**, *8*, 305–320. [[CrossRef](#)]
16. Stütz, A.E.; Paulsen, H. *Iminosugars as Glycosidase Inhibitors*; Wiley-VCH Verlag GmbH: Hoboken, NJ, USA, 1998.
17. Kumar Thakur, A.; Kumar, Y.; K Goyal, K. Pharmacotherapeutics of miglitol: An  $\alpha$ -glucosidase inhibitor. *J. Anal. Pharm. Res.* **2018**, *7*, 617–619. [[CrossRef](#)]
18. Hollak, C.E.M.; Hughes, D.; van Schaik, I.N.; Schwierin, B.; Bembi, B. Miglustat (Zavesca®) in type 1 Gaucher disease: 5-year results of a post-authorisation safety surveillance programme. *Pharmacoepidemiol. Drug Saf.* **2009**, *18*, 770–777. [[CrossRef](#)]

19. Patterson, M.C.; Mengel, E.; Vanier, M.T.; Moneuse, P.; Rosenberg, D.; Pineda, M. Treatment outcomes following continuous miglustat therapy in patients with Niemann-Pick disease Type C: A final report of the NPC Registry. *Orphanet J. Rare Dis.* **2020**, *15*, 104. [CrossRef] [PubMed]
20. Riccio, E.; Zanfardino, M.; Ferreri, L.; Santoro, C.; Cocozza, S.; Capuano, I.; Imbriaco, M.; Feriozzi, S.; Pisani, A. Switch from enzyme replacement therapy to oral chaperone migalastat for treating Fabry disease: Real-life data. *Eur. J. Hum. Genet.* **2020**, *28*, 1662–1668. [CrossRef] [PubMed]
21. Jenkinson, S.F.; Fleet, G.W.J.; Nash, R.J.; Koike, Y.; Adachi, I.; Yoshihara, A.; Morimoto, K.; Izumori, K.; Kato, A. Looking-glass synergistic pharmacological chaperones: DGJ and L-DGJ from the enantiomers of tagatose. *Org. Lett.* **2011**, *13*, 4064–4067. [CrossRef] [PubMed]
22. D’Alonzo, D.; De Fenza, M.; Porto, C.; Iacono, R.; Huebecker, M.; Cobucci-Ponzano, B.; Priestman, D.A.; Platt, F.; Parenti, G.; Moracci, M.; et al. N-Butyl-L-deoxynojirimycin (L-NBDN): Synthesis of an allosteric enhancer of  $\alpha$ -glucosidase activity for the treatment of Pompe disease. *J. Med. Chem.* **2017**, *60*. [CrossRef] [PubMed]
23. De Fenza, M.; D’Alonzo, D.; Esposito, A.; Munari, S.; Loberto, N.; Santangelo, A.; Lampronti, I.; Tamanini, A.; Rossi, A.; Ranucci, S.; et al. Exploring the effect of chirality on the therapeutic potential of N-alkyl-deoxyiminosugars: Anti-inflammatory response to *Pseudomonas aeruginosa* infections for application in CF lung disease. *Eur. J. Med. Chem.* **2019**, *175*, 63–71. [CrossRef] [PubMed]
24. Esposito, A.; D’Alonzo, D.; De Fenza, M.; De Gregorio, E.; Tamanini, A.; Lippi, G.; Dececchi, M.C.; Guaragna, A. Synthesis and therapeutic applications of iminosugars in cystic fibrosis. *Int. J. Mol. Sci.* **2020**, *21*, 3353. [CrossRef] [PubMed]
25. Shibano, M.; Tsukamoto, D.; Masuda, A.; Tanka, Y.; Kusano, G. Two new pyrrolidine alkaloids, radicamines A and B, as inhibitors of alpha-glucosidase from lobelia chinensis Lour. *Chem. Pharm. Bull.* **2001**, *49*, 1362–1365. [CrossRef] [PubMed]
26. Haarr, M.B.; Lopéz, Ó.; Pejov, L.; Fernández-Bolaños, J.G.; Lindbäck, E.; Sydnes, M.O. 1,4-Dideoxy-1,4-imino-D-arabinitol (DAB) analogues possessing a hydrazide imide moiety as potent and selective  $\alpha$ -mannosidase inhibitors. *ACS Omega* **2020**, *5*, 18507–18514. [CrossRef] [PubMed]
27. Asano, N.; Oseki, K.; Kizu, H.; Matsui, K. Nitrogen-in-the-ring pyranoses and furanoses: Structural basis of inhibition of mammalian glycosidases. *J. Med. Chem.* **1994**, *37*, 3701–3706. [CrossRef]
28. Evans, G.; Schramm, V.; Tyler, P. The immucillins: Design, synthesis and application of transition-state analogues. *Curr. Med. Chem.* **2015**, *22*. [CrossRef]
29. Evans, G.B.; Tyler, P.C.; Schramm, V.L. Immucillins in infectious diseases. *ACS Infect. Dis.* **2018**, *4*, 107–117. [CrossRef]
30. Lim, S.-Y.; Osuna, C.E.; Best, K.; Taylor, R.; Chen, E.; Yoon, G.; Kublin, J.L.; Schalk, D.; Schultz-Darken, N.; Capuano, S.; et al. A direct-acting antiviral drug abrogates viremia in Zika virus-infected rhesus macaques. *Sci. Transl. Med.* **2020**, *12*, eaau9135. [CrossRef]
31. Warren, T.K.; Wells, J.; Panchal, R.G.; Stuthman, K.S.; Garza, N.L.; Van Tongeren, S.A.; Dong, L.; Retterer, C.J.; Eaton, B.P.; Pegoraro, G.; et al. Protection against filovirus diseases by a novel broad-spectrum nucleoside analogue BCX4430. *Nature* **2014**, *508*, 402–405. [CrossRef]
32. Elfiky, A.A. Ribavirin, Remdesivir, Sofosbuvir, Galidesivir, and Tenofovir against SARS-CoV-2 RNA dependent RNA polymerase (RdRp): A molecular docking study. *Life Sci.* **2020**, *253*, 117592. [CrossRef]
33. A Study to Evaluate the Safety, Pharmacokinetics and Antiviral Effects of Galidesivir in Yellow Fever or COVID-19; last update: July 23, 2020. Start Date: April 2020. Available online: <https://clinicaltrials.gov/ct2/show/NCT03891420> (accessed on 17 November 2020).
34. Kicska, G.A.; Long, L.; Horig, H.; Fairchild, C.; Tyler, P.C.; Furneaux, R.H.; Schramm, V.L.; Kaufman, H.L. Immucillin H, a powerful transition-state analog inhibitor of purine nucleoside phosphorylase, selectively inhibits human T lymphocytes. *Proc. Natl. Acad. Sci. USA* **2001**, *98*, 4593–4598. [CrossRef] [PubMed]
35. Evans, G.B.; Schramm, V.L.; Tyler, P.C. The transition to magic bullets—transition state analogue drug design. *Medchemcomm* **2018**, *9*, 1983–1993. [CrossRef]
36. Gandhi, V.; Kilpatrick, J.M.; Plunkett, W.; Ayres, M.; Harman, L.; Du, M.; Bantia, S.; Davisson, J.; Wierda, W.G.; Faderl, S.; et al. A proof-of-principle pharmacokinetic, pharmacodynamic, and clinical study with purine nucleoside phosphorylase inhibitor immucillin-H (BCX-1777, forodesine). *Blood* **2005**, *106*, 4253–4260. [CrossRef]
37. Ho, M.-C.; Shi, W.; Rinaldo-Matthis, A.; Tyler, P.C.; Evans, G.B.; Clinch, K.; Almo, S.C.; Schramm, V.L. Four generations of transition-state analogues for human purine nucleoside phosphorylase. *Proc. Natl. Acad. Sci. USA* **2010**, *107*, 4805–4812. [CrossRef] [PubMed]
38. Le, B.T.; Chen, S.; Abramov, M.; Herdewijn, P.; Veedu, R.N. Evaluation of anhydrohexitol nucleic acid, cyclohexenyl nucleic acid and D-altritol nucleic acid-modified 2'-O-methyl RNA mixmer antisense oligonucleotides for exon skipping in vitro. *Chem. Commun.* **2016**, *52*, 13467–13470. [CrossRef]
39. De Fenza, M.; Eremeeva, E.; Troisi, R.; Yang, H.; Esposito, A.; Sica, F.; Herdewijn, P.; D’Alonzo, D.; Guaragna, A. Structure—activity relationship study of a potent  $\alpha$ -thrombin binding aptamer incorporating hexitol nucleotides. *Chem. A Eur. J.* **2020**, *26*, 9589–9597. [CrossRef]
40. Herdewijn, P. Nucleic acids with a six-membered ‘carbohydrate’ mimic in the backbone. *Chem. Biodivers.* **2010**, *7*, 1–59. [CrossRef] [PubMed]
41. D’Alonzo, D.; Amato, J.; Schepers, G.; Froeyen, M.; Van Aerschot, A.; Herdewijn, P.; Guaragna, A. Enantiomeric selection properties of  $\beta$ -homodNA: Enhanced pairing for heterochiral complexes. *Angew. Chem. Int. Ed.* **2013**, *52*, 6662–6665. [CrossRef]

42. Paoletta, C.; D'Alonzo, D.; Schepers, G.; Van Aerschot, A.; Di Fabio, G.; Palumbo, G.; Herdewijn, P.; Guaragna, A. Oligonucleotides containing a *ribo*-configured cyclohexanyl nucleoside: Probing the role of sugar conformation in base pairing selectivity. *Org. Biomol. Chem.* **2015**, *13*, 10041–10049. [[CrossRef](#)] [[PubMed](#)]
43. D'Alonzo, D.; Froeyen, M.; Schepers, G.; Di Fabio, G.; Van Aerschot, A.; Herdewijn, P.; Palumbo, G.; Guaragna, A. 1',5'-Anhydro-L-*ribo*-hexitol adenine nucleic acids ( $\alpha$ -L-HNA-A): Synthesis and chiral selection properties in the mirror image world. *J. Org. Chem.* **2015**, *80*, 5014–5022. [[CrossRef](#)]
44. Esposito, A.; Giovanni, C.; De Fenza, M.; Talarico, G.; Chino, M.; Palumbo, G.; Guaragna, A.; D'Alonzo, D. A stereoconvergent Tsuji–Trost reaction in the synthesis of cyclohexenyl nucleosides. *Chem. -Eur. J.* **2020**, *26*, 2597–2601. [[CrossRef](#)]
45. Oliviero, G.; Amato, J.; Borbone, N.; D'Errico, S.; Piccialli, G.; Mayol, L. Synthesis of N-1 and ribose modified inosine analogues on solid support. *Tetrahedron Lett.* **2007**, *48*, 397–400. [[CrossRef](#)]
46. Oliviero, G.; Amato, J.; Borbone, N.; D'Errico, S.; Piccialli, G.; Bucci, E.; Piccialli, V.; Mayol, L. Synthesis of 4-N-alkyl and ribose-modified AICAR analogues on solid support. *Tetrahedron* **2008**, *64*, 6475–6481. [[CrossRef](#)]
47. Guaragna, A.; D'Errico, S.; D'Alonzo, D.; Pedatella, S.; Palumbo, G. A general approach to the synthesis of 1-deoxy-L-imosugars. *Org. Lett.* **2007**, *9*, 3473–3476. [[CrossRef](#)]
48. Böshagen, H.; Heiker, F.-R.; Matthias Schüller, A. The chemistry of the 1-deoxynojirimycin system. Synthesis of 2-acetamido-1,2-dideoxynojirimycin from 1-deoxynojirimycin. *Carbohydr. Res.* **1987**, *164*, 141–148. [[CrossRef](#)]
49. Pedatella, S.; Guaragna, A.; D'Alonzo, D.; De Nisco, M.; Palumbo, G. Triphenylphosphine polymer-bound/iodine complex: A suitable reagent for the preparation of *O*-isopropylidene sugar derivatives. *Synthesis* **2006**, 305–308. [[CrossRef](#)]
50. Guaragna, A.; Amoresano, A.; Pinto, V.; Monti, G.; Mastrobuoni, G.; Marino, G. Synthesis and proteomic activity evaluation of a new isotope-coded affinity tagging (ICAT) reagent. *Bioconjug. Chem.* **2008**, *19*, 1095–1104. [[CrossRef](#)]
51. Esposito, A.; De Gregorio, E.; De Fenza, M.; D'Alonzo, D.; Satawani, A.; Guaragna, A. Expeditious synthesis and preliminary antimicrobial activity of deflazacort and its precursors. *RSC Adv.* **2019**, *9*, 21519–21524. [[CrossRef](#)]
52. De Gregorio, E.; Esposito, A.; Vollaro, A.; De Fenza, M.; D'Alonzo, D.; Migliaccio, A.; Iula, V.D.; Zarrilli, R.; Guaragna, A. N-Nonyloxypropyl-L-deoxynojirimycin inhibits growth, biofilm formation and virulence factors expression of *Staphylococcus aureus*. *Antibiotics* **2020**, *9*, 362. [[CrossRef](#)] [[PubMed](#)]
53. Esposito, A.; D'Alonzo, D.; D'Errico, S.; De Gregorio, E.; Guaragna, A. Toward the identification of novel antimicrobial agents: One-pot synthesis of lipophilic conjugates of N-alkyl D- and L-imosugars. *Mar. Drugs* **2020**, *18*, 572. [[CrossRef](#)]
54. Moussa, Z.; Judeh, Z.M.A.; Ahmed, S.A. Polymer-supported triphenylphosphine: Application in organic synthesis and organometallic reactions. *RSC Adv.* **2019**, *9*, 35217–35272. [[CrossRef](#)]
55. D'Alonzo, D.; Guaragna, A.; Palumbo, G. Exploring the role of chirality in nucleic acid recognition. *Chem. Biodivers.* **2011**, *8*, 373–413. [[CrossRef](#)] [[PubMed](#)]
56. Maurinsh, Y.; Rosemeyer, H.; Esnouf, R.; Medvedovici, A.; Wang, J.; Ceulemans, G.; Lescrier, E.; Hendrix, C.; Busson, R.; Sandra, P.; et al. Synthesis and pairing properties of oligonucleotides containing 3-hydroxy-4-hydroxymethyl-1-cyclohexanyl nucleosides. *Chem. Eur. J.* **1999**, *5*, 2139–2150. [[CrossRef](#)]
57. Rengasamy, R.H.; Curtis-Long, M.J.; Ryu, H.W.; Oh, K.Y.; Park, K.H. Stereoselective synthesis of L-deoxyaltronojirimycin from L-serine. *Bull. Korean Chem. Soc.* **2009**, *30*, 1531–1534. [[CrossRef](#)]